

Towards a unified realistic shell-model Hamiltonian with the monopole-based universal force

K. Kaneko¹, T. Mizusaki², Y. Sun^{3,4}, S. Tazaki⁵

¹Department of Physics, Kyushu Sangyo University, Fukuoka 813-8503, Japan

²Institute of Natural Sciences, Senshu University, Tokyo 101-8425, Japan

³Department of Physics and Astronomy, Shanghai Jiao Tong University, Shanghai 200240, People's Republic of China

⁴Institute of Modern Physics, Chinese Academy of Sciences, Lanzhou 730000, People's Republic of China

⁵Department of Applied Physics, Fukuoka University, Fukuoka 814-0180, Japan

(Dated: September 6, 2018)

We propose a unified realistic shell-model Hamiltonian employing the pairing plus multipole Hamiltonian combined with the monopole interaction constructed starting from the monopole-based universal force by Otsuka *et al.* (Phys. Rev. Lett. 104, 012501 (2010)). It is demonstrated that the proposed PMMU model can consistently describe a large amount of spectroscopic data as well as binding energies in the pf and $pf_{5/2g_{9/2}}$ shell spaces, and could serve as a practical shell model for even heavier mass regions.

PACS numbers: 21.30.Fe, 21.60.Cs, 21.10.Dr, 27.50.+e

The nuclear shell-model interaction can in principle be derived microscopically from the free nucleon-nucleon force. In fact, such attempts were made in the early years for the beginning of the shell [1, 2]. However, it was soon after realized that such an interaction fail to describe binding energies, excitation spectra, and transitions if many valence nucleons were considered. To reproduce experimental data, considerable efforts have been put forward to construct the so-called effective interactions, such as USD [3] and USDA/B [4] for the sd shell, KB3G [5] and GXPF1A [6] for the pf shell, and JUN45 [7] and jj4b [8] for the $pf_{5/2g_{9/2}}$ model space. Each of these interactions is applicable to a given model space while mutual relations among them are obscure. On the other hand, it has been shown [9] that realistic effective interactions are dominated by the pairing plus quadrupole-quadrupole ($P + QQ$) terms with the monopole interaction. This finding not only makes the understanding of effective interactions in nuclei intuitive, but may also be used to unify effective interactions for different model spaces. In particular, one may begin to talk about universality for shell models.

Along the lines of this thought, we have carried out shell-model calculations using the extended $P + QQ$ Hamiltonian combined with the monopole terms ($EPQQM$), which are regarded as corrections for the average monopole interaction. It has been demonstrated that despite of its simplicity, this $EPQQM$ model works surprisingly well for different mass regions, for example, the proton-rich pf shell [10] and the $pf_{5/2g_{9/2}}$ shell [11], the neutron-rich fpg shell [12], and the sd - pf shell region [13]. It has also been successfully applied to the neutron-rich nuclei around ^{132}Sn [14, 15]. However, these calculations rely heavily on phenomenological adjustments on the monopole corrections. Consequently, the $EPQQM$ model cannot describe binding energies or unusual structures such as the first excited 0^+ state of Zn and Ge isotopes around $N = 40$ [16], and it essentially provides no information about the unconventional shell evolution in neutron-rich nuclei.

The monopole interaction is a crucial ingredient for suc-

cessful shell-model calculations. It is defined as [17]

$$V_m(ab, T) = \frac{\sum_J (2J+1) V_{ab,ab}^{JT}}{\sum_J (2J+1)}, \quad (1)$$

where $V_{ab,ab}^{JT}$ are the interaction matrix elements. The connection between the monopole interaction and the tensor force [18] was confirmed, which explains the shell evolution [19]. It was shown [20, 21] that also three-nucleon forces are important for the monopole interaction between valence neutrons. Recently, novel general properties of the monopole components in the effective interaction have been demonstrated by Otsuka *et al.* by introducing the monopole-based universal

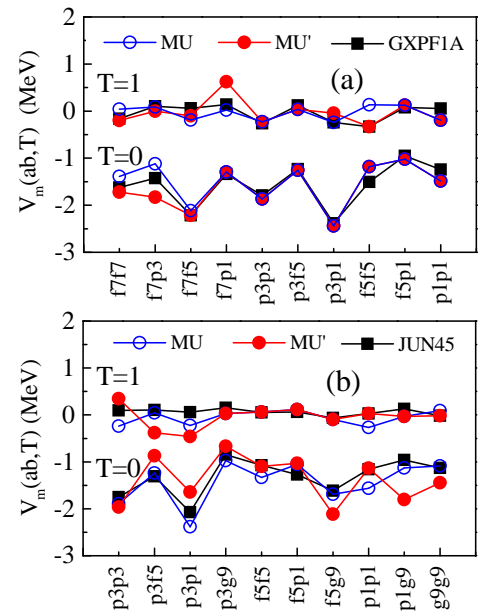


FIG. 1: (Color online) Monopole matrix elements for (a) pf and (b) $pf_{5/2g_{9/2}}$ model space. The original V_m^{MU} and modified $V_m^{MU'}$ are shown by open and full circles, respectively. The monopole matrix elements of the GXPF1A interaction [6] for pf shell and JUN45 [7] for $pf_{5/2g_{9/2}}$ shell are also shown for comparison. For orbital labels, "f7p3", for example, stands for $a = f_{7/2}$ and $b = p_{3/2}$.

force V_{MU} [22], which consists of the Gaussian central force and the tensor force. The proposed force has been successfully applied to light nuclei [23, 24]. As seen in Fig. 1, the monopole matrix elements V_m^{MU} obtained from this force are very similar to those of the GXPF1A interaction [6] for the pf and JUN45 [7] for the $pf_{5/2}g_{9/2}$ shell space. This let us to speculate that the V_{MU} force proposed in Ref. [22] would be universal, maybe applicable to different mass regions. Thus it is of great interest to investigate the applicability of V_{MU} by carrying out large-scale shell-model calculations for nuclei in medium-mass regions. In this Rapid Communication, we show that the monopole interaction derived from the monopole-based unified force [22], with refitting some monopole terms in accordance with each of the model spaces, works well as an important part of a unified effective Hamiltonian for the pf and $pf_{5/2}g_{9/2}$ spaces. The conclusion is supported by a systematical study of binding energies and by performing detailed spectroscopic calculations for a wide range of nuclei.

Our proposed Hamiltonian combines the pairing plus multipole terms with the monopole interaction V_m^{MU} (hereafter termed the PMMU model)

$$\begin{aligned}
 H &= H_0 + H_{PM} + H_m^{MU}, \quad (2) \\
 H_0 &= \sum_{\alpha} \varepsilon_{\alpha} c_{\alpha}^{\dagger} c_{\alpha}, \\
 H_{PM} &= - \sum_{J=0,2} \frac{1}{2} g_J \sum_{M\kappa} P_{JM1\kappa}^{\dagger} P_{JM1\kappa} \\
 &\quad - \frac{1}{2} \chi_2 \sum_M : Q_{2M}^{\dagger} Q_{2M} : - \frac{1}{2} \chi_3 \sum_M : O_{3M}^{\dagger} O_{3M} : \\
 H_m^{MU} &= \sum_{a \leq b, T} V_m^{MU}(ab, T) \sum_{JMK} A_{JMTK}^{\dagger}(ab) A_{JMTK}(ab).
 \end{aligned}$$

For the pairing plus multipole part, we take the $J = 0, 2$ terms in the particle-particle channel and the quadrupole-quadrupole (QQ) and octupole-octupole (OO) terms in the particle-hole channel [10, 11]. (Higher order pairing and multipole terms can be added if necessary.) We adopt the monopole matrix elements constructed from the monopole-based universal force [22], in which the Gaussian parameter is fixed as $\mu = 1.0$ fm, and the strength parameters used here are the same as those in Ref. [22]. The harmonic oscillator basis with $\hbar\omega = 41A^{-1/3}$ is used in the calculation of the matrix elements. Note that in the monopole Hamiltonian given above, $V_m^{MU}(ab, T)$ is the modified one labeled as MU' in Fig. 1. It should be emphasized that the monopole interaction V_m^{MU} is a part of the effective interaction in the present model, not just a correction as treated in our previous papers (see, for example, Ref. [16]). In this way, effective single-particle energies are crucially improved to reflect the shell evolution.

Shell-model calculations are performed with the code MSHELL64 [25]. We first apply the PMMU model in the pf model space. The calculated total binding energy is obtained by adding an appropriate Coulomb energy to the shell-model

ground-state energy. In the pf -shell calculation, Coulomb energies are evaluated as in Ref. [26] by using an empirical formula $E_C = V_{pp}p(p-1) + V_{pn}pn + e_p p$, where p (n) denotes the number of valence protons (neutrons) and the adopted parameters are $V_{pp} = 0.10$, $V_{pn} = -0.203$, and $e_p = 6.90$ (all in MeV). Data from 95 nuclei [27], $^{42-49}\text{Ca}$, $^{43-54}\text{Sc}$, $^{48-55}\text{Ti}$, $^{50-60}\text{V}$, $^{51-62}\text{Cr}$, $^{52-63}\text{Mn}$, $^{53-64}\text{Fe}$, $^{54-64}\text{Co}$, and $^{56-64}\text{Ni}$, are taken for fitting. All the results for Ca, Sc, Ti, and Cr isotopes are obtained without any truncation. For the other isotopes, the maximal number of allowed particles excited from the $f_{7/2}$ orbital is limited. The rms deviation for binding energies is 707 keV. As a result, the interaction strengths in (2) are determined to be $g_0 = 20.2/A$, $g_2 = 228.2/A^{5/3}$, $\chi_2 = 228.2/A^{5/3}$, and $\chi_3 = 0.0$, and the single-particle energies to be $\varepsilon_{f_{7/2}} = -7.78$, $\varepsilon_{p_{3/2}} = -5.68$, $\varepsilon_{f_{5/2}} = -1.28$, and $\varepsilon_{p_{1/2}} = -3.88$ (all in MeV). For the pf shell, 10 monopole terms are also modified for fitting. The results are displayed as $V_m^{MU'}$ in Fig. 1(a). All the monopole matrix elements are scaled with a factor $(42/A)^{0.3}$ in the calculation.

Our strength parameters g_0 and χ_2 agree, respectively, with $g_0 = 20/A$ and $\chi_2 = 240/A^{5/3}$ of Bes and Sorensen [28]. We may also compare our strengths with those derived from the GXPF1A interaction using the prescription of Dufour and Zuker [9]. They can be estimated from the following equations; $g_0 = |E^{01}| \frac{\hbar\omega}{\hbar\omega_0} \Omega_r^{-1}$ and $\chi_2 = 2|e^{20}| \frac{\hbar\omega}{\hbar\omega_0} N_r^{-2}$, where E^{JT} and e^{JT} are, respectively, E - and e -eigenvalues, and $\Omega_r = 0.655A^{2/3}$, $N_r^2 = 0.085A^{4/3}$, $\hbar\omega = 40A^{-1/3}$, and $\hbar\omega_0 = 9.0$ (see Ref. [9]). The E -eigenvalue of the interaction matrix for $J = 0, T = 1$ is $E^{01} = -4.18$, and the e -eigenvalue for $J = 2, T = 0$ particle-hole channel is $e^{20} = -2.92$ [6]. The obtained strength parameters using the above values are $g_0 = 28.4/A$ and $\chi_2 = 305.4/A^{5/3}$. A comparison of these values with the strength parameters determined from our calculation reveals that both have the same mass dependence while ours are about 0.73 times smaller than those of GXPF1A. This result is interesting because it indicates that the GXPF1A model and our PMMU model for the pf shell are different, but may be closely related.

In Fig. 2, the results from calculations with the PMMU Hamiltonian are compared with available experimental data for the pf shell nuclei. The left panel of Fig. 2 shows excitation energies of the 2_1^+ state for Ca, Ti, Cr, Fe, and Ni isotopes. The systematic behavior of the 2_1^+ energy levels is reasonably described for these isotopes although the calculation produces a small jump corresponding to the shell closure at $N = 32$ for the Ca and Ni isotopes. At $N = 40$, deviations from the experimental levels are seen. Especially, the calculated 2_1^+ for ^{58}Ca and ^{66}Ni are quite large, which may indicate that the $g_{9/2}$ orbital could be important for these levels. In the middle panel, calculated $B(E2; 2_1^+ \rightarrow 0_1^+)$ values are shown, for which the effective charges are taken as $e_p = 1.5e$ and $e_n = 0.5e$. The calculation basically accounts for the variation trend, however with deviations from data for the beginning and end of the shell. For Ca nuclei with $N \leq 24$ and Ni nuclei with $N \geq 32$, the calculated $B(E2)$ values are smaller than experiment. The

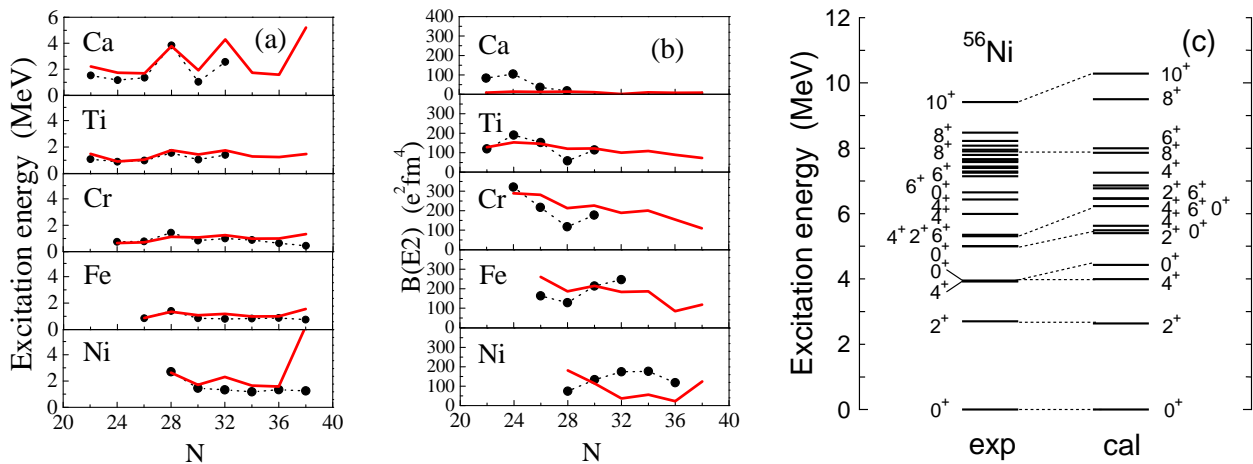


FIG. 2: (Color online) Systematics for pf -shell nuclei. (Left panel) 2_1^+ energy, (middle panel) $B(E2; 2_1^+ \rightarrow 0_1^+)$ value, and (right panel) energy spectrum for ^{56}Ni . Filled circles and solid lines in the left and middle panels indicate experimental data and the calculated results, respectively. The experimental data are taken from [29].

reason for the deviations is understandable. Those in Ca may suggest that the contribution of core excitations from the sd shell is large and those in Ni may indicate that inclusion of the $g_{9/2}$ and $d_{5/2}$ orbitals in the model space is important. As an example of detailed spectroscopic calculations, the obtained energy levels for ^{56}Ni are compared with data in the right panel. It can be seen that the calculation reproduces the data very well. In particular, the agreement with the experimental levels below 5 MeV is excellent. Experimental information for electromagnetic transitions is rather limited for this nucleus. The calculated values $B(E2; 2_1^+ \rightarrow 0_1^+) = 181.2 e^2\text{fm}^2$ and $B(E2; 4_1^+ \rightarrow 2_1^+) = 121.0 e^2\text{fm}^2$ are compared with experimental ones [30] $120 \pm 24 e^2\text{fm}^2$ and $< 305 e^2\text{fm}^2$, respectively.

Next we apply the PMMU model for the $pf_{5/2}g_{9/2}$ -space. Binding energies are evaluated by using the empirical formula for the Coulomb energy with the parameter set 2 given in Table I of Ref. [31]. The data from 91 nuclei, $^{64-76}\text{Ni}$, $^{64-78}\text{Cu}$, $^{65-80}\text{Zn}$, $^{66-80}\text{Ga}$, $^{69-80}\text{Ge}$, $^{67-78}\text{As}$, and $^{73-80}\text{Se}$ [27], are taken for the fitting calculation. For Ni, Cu, Zn, Ga, and Ge isotopes, the calculation is performed without any truncation, while for As and Se isotopes, some truncations are introduced. The rms deviation for binding energies is 691 keV. The resulting interaction strengths in Eq. (2) are $g_0 = 18.0/A$, $g_2 = 0.0$, $\chi_2 = 334.0/A^{5/3}$, and $\chi_3 = 259.2/A^2$, and the single-particle energies are $\varepsilon_{p3/2} = -9.40$, $\varepsilon_{f5/2} = -8.29$, $\varepsilon_{p1/2} = -7.49$, and $\varepsilon_{g9/2} = -5.70$ (all in MeV). For this shell space, 14 monopole terms are modified for fitting, with the results displayed as V_m^{MU} in Fig. 1(b). All the monopole matrix elements are scaled with a factor $(58/A)^{0.3}$ in the calculation.

In Fig. 3, we show the results for Ni, Zn, Ge, and Se isotopes. $E_x(2_1^+)$ and $B(E2; 2_1^+ \rightarrow 0_1^+)$ values are compared with experimental data in the left and middle panel, respectively. The effective charges are taken as $e_p = 1.5e$ and $e_n = 1.1e$. For Zn isotopes, both $E_x(2_1^+)$ and $B(E2)$ are described reasonably

well. Near $N = 40$, the calculated $B(E2)$ values nevertheless underestimate the data. The calculation also reproduces well the experimental data for Ge and Se isotopes. The feature that $B(E2)$ values for both isotopic chains increase around $N = 44$ is correctly described. For Ge isotopes, the overall agreement in $E_x(2_1^+)$ is obtained. The calculated $B(E2)$ values are however found too large for $^{66,68}\text{Ge}$, which was also seen in the JUN45 calculation [7]. It was pointed out [32] that these experimental $B(E2)$ values can be reproduced if a smaller neutron effective charge $e_n = 0.5e$ is used. Thus this problem currently remains as an open question. Finally for Ni isotopes, the observed 2_1^+ energy shows the largest value at $N = 40$ while the calculation suggests the largest at $N = 38$. For all the Ni isotopes the calculated $E_x(2_1^+)$ are somewhat higher than experiment and the $B(E2)$ values are smaller. The problem with the present calculation may be the restriction in the $pf_{5/2}g_{9/2}$ -shell space without inclusion of the $f_{7/2}$ and $d_{5/2}$ orbitals.

^{72}Ge is an interesting nucleus because its first excited 0^+ state is found to be the lowest in all the Ge isotopes, which lies below 2_1^+ . As one can see from the right panel of Fig. 3, this feature is correctly reproduced by the present calculation. It is remarkable that the calculation shows a one-to-one correspondence with experimental levels for positive-parity states up to high excitations. The calculated $B(E2; 2_1^+ \rightarrow 0_1^+) = 462.0 e^2\text{fm}^2$ and $B(E2; 4_1^+ \rightarrow 2_1^+) = 712.1 e^2\text{fm}^2$ are compared well with the experimental data $418.1 \pm 72 e^2\text{fm}^2$ and $658.3 \pm 88 e^2\text{fm}^2$ [29], respectively.

Description of odd-nuclei is generally a challenging task for shell-model calculations. To further test the PMMU model, we take ^{55}Co and ^{69}Ge as examples for the pf and $pf_{5/2}g_{9/2}$ shell spaces, respectively. As one can see in Fig. 4, the present model works well also for odd-mass nuclei. If one assumes an inert ^{56}Ni core, the low-lying states of ^{55}Co may be naively understood so as to be built by the simple $f_{7/2}$

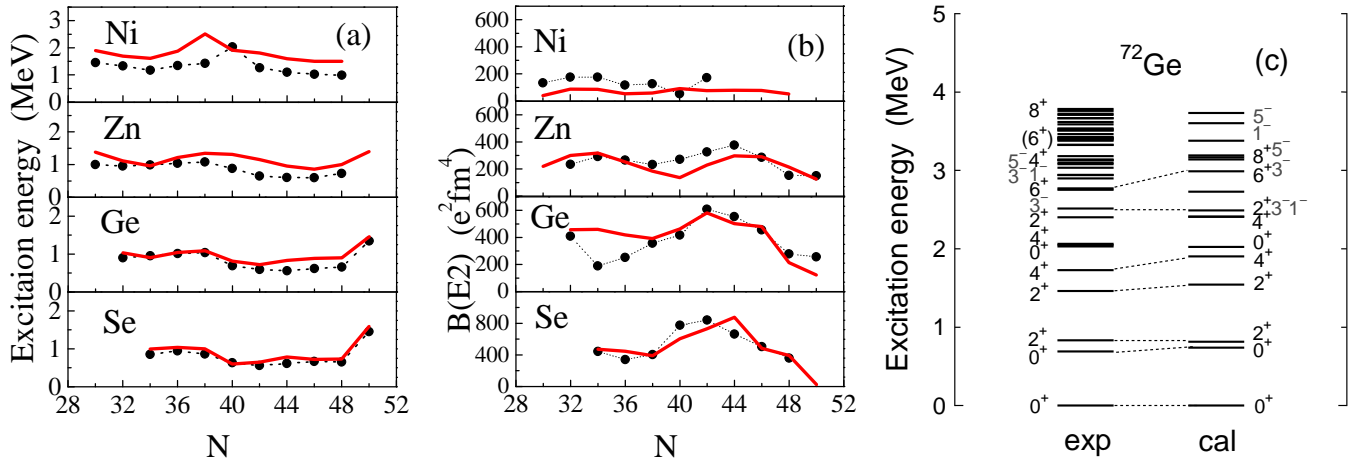


FIG. 3: (Color online) Systematics for $pf_{5/2}g_{9/2}$ -shell nuclei. (Left panel) 2_1^+ energy, (middle panel) $B(E2; 2_1^+ \rightarrow 0_1^+)$ value, and (right panel) energy spectrum for ^{72}Ge . Filled circles and solid lines in the left and middle panels indicate experimental data and the calculated results, respectively. The experimental data are taken from [29].

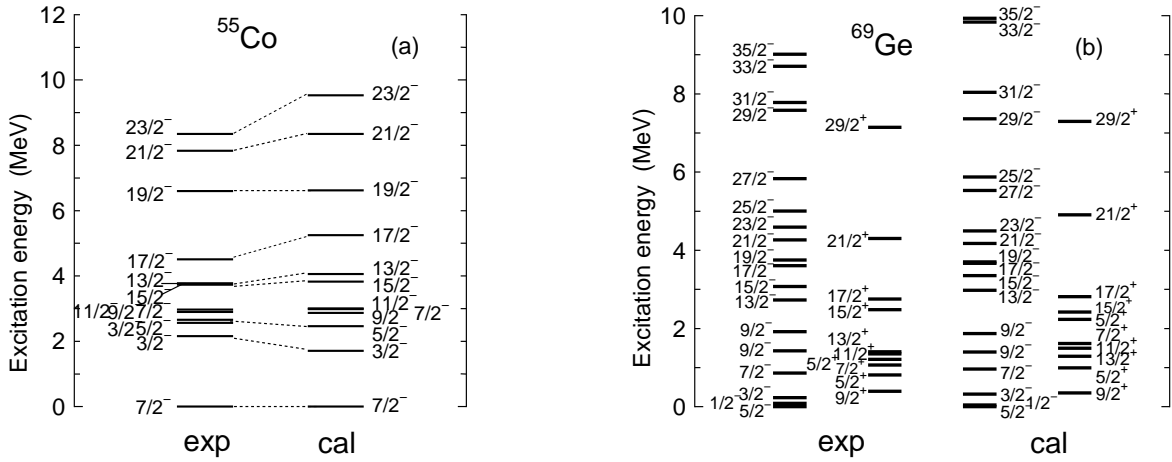


FIG. 4: Calculated energy levels for ^{55}Co and ^{69}Ge are compared with the corresponding experimental data taken from [29].

proton-hole configuration, having $7/2^-$ as the ground state. However, our calculation indicates that for the yrast states up to $17/2^-$, the ^{56}Ni core is strongly broken and excitations from the $f_{7/2}$ orbital to the upper pf -shell are large. The higher spin $13/2^-$, $15/2^-$, and $17/2^-$ states are described mainly by neutron excitations. For ^{69}Ge , agreement of the calculation with data is excellent for both negative- and positive-parity states. In particular, the calculation reproduces well the low-lying states including the ground state $5/2^-$. Discrepancies in the ^{69}Ge calculation are found for the $25/2^-$, $33/2^-$, and $35/2^-$ states, for which the theoretical levels lie by about 1 MeV higher than the experimental data.

Although the present PMMU is constructed very differently from the GXPF1A or JUN45 shell model, the striking similarities in their monopole matrix elements shown in Fig. 1 ensure that they may describe shell structures equally well. We have found that the monopole matrix elements in USD and USDA/B are also quite similar to those in PMMU. However,

the merit of PMMU is that its interaction takes a very simple form with a common mass dependence for different mass regions and has a much smaller number of parameters in the Hamiltonian. One may expect that the model works even better for heavier nuclei because the $P+QQ$ type of forces is well justified there. This may open a promising path for shell models to be consistently applied to heavy systems, for example, the $A \sim 100$ mass region.

In conclusion, we have made a step towards a unification of effective shell-model Hamiltonian applicable to different mass regions. The Hamiltonian adopts the well-established pairing-plus-multipole force and is crucially combined with the monopole interaction derived from the recently-proposed monopole-based universal force [22]. The constructed PMMU model has been applied to a large number of nuclei in the pf and $pf_{5/2}g_{9/2}$ shell regions. For both regions, the PMMU model, with the resulting force strengths and the scaling parameters with a common mass dependence adjusted to

systematical reproduction of binding energies, can well describe the experimental spectra and transitions, for both the near-ground-state region and high-spin excitations. It has been suggested that the PMMU model could be a feasible method to unify different shell models so that one may extend shell-model calculations to heavier systems.

Research at SJTU was supported by the National Natural Science Foundation of China (Nos. 11135005 and 11075103) and by the 973 Program of China (No. 2013CB834401).

-
- [1] T. T. S. Kuo and G. E. Brown, Nucl. Phys. A **114**, 241 (1968).
 [2] M. Hjorth-Jensen, T. T. S. Kuo, and E. Osnes, Phys. Rep. **261**, 125 (1995).
 [3] B. A. Brown and B. H. Wildenthal, Ann. Rev. Nucl. Part. Sci. **38**, 29 (1988).
 [4] B. A. Brown and W. A. Richter, Phys. Rev. C **74**, 034315 (2006).
 [5] A. Poves, J. Sanchez-Solano, E. Caurier, and F. Nowacki, Nucl. Phys. A **694**, 157 (2001).
 [6] M. Honma, T. Otsuka, B. A. Brown, and T. Mizusaki, Phys. Rev. C **69**, 034335 (2004).
 [7] M. Honma, T. Otsuka, T. Mizusaki, and M. Hjorth-Jensen, Phys. Rev. C **80**, 064323 (2009).
 [8] B. A. Brown and A. F. Lisetskiy (unpublished).
 [9] M. Dufour and A. P. Zuker, Phys. Rev. C **54**, 1641 (1996).
 [10] M. Hasegawa, K. Kaneko, and S. Tazaki, Nucl. Phys. A **688**, 765 (2001).
 [11] K. Kaneko, M. Hasegawa, and T. Mizusaki, Phys. Rev. C **66**, 051306(R) (2002).
 [12] K. Kaneko, Y. Sun, M. Hasegawa, and T. Mizusaki, Phys. Rev. C **78**, 064312 (2008).
 [13] K. Kaneko, Y. Sun, M. Hasegawa, and T. Mizusaki, Phys. Rev. C **83**, 014320 (2011).
 [14] H. Jin, M. Hasegawa, S. Tazaki, K. Kaneko, and Y. Sun, Phys. Rev. C **84**, 044324 (2011).
 [15] H.-K. Wang, Y. Sun, H. Jin, K. Kaneko, and S. Tazaki, Phys. Rev. C **88**, 054310 (2013).
 [16] M. Hasegawa, T. Mizusaki, K. Kaneko, and Y. Sun, Nucl. Phys. A **789**, 46 (2007).
 [17] A. Poves and A. Zuker, Phys. Rep. **70**, 235 (1981).
 [18] T. Otsuka, R. Fujimoto, Y. Utsuno, B. A. Brown, M. Honma, and T. Mizusaki, Phys. Rev. Lett. **87**, 082502 (2001).
 [19] T. Otsuka, T. Suzuki, R. Fujimoto, H. Grawe, and Y. Akaishi, Phys. Rev. Lett. **95**, 232502 (2005).
 [20] A. P. Zuker, Phys. Rev. Lett. **90**, 042502 (2003).
 [21] T. Otsuka, T. Suzuki, J. D. Holt, A. Schwenk, and Y. Akaishi, Phys. Rev. Lett. **105**, 032501 (2010).
 [22] T. Otsuka, T. Suzuki, M. Honma, Y. Utsuno, N. Tsunoda, K. Tsukiyama, and M. Hjorth-Jensen, Phys. Rev. Lett. **104**, 012501 (2010).
 [23] C. Yuan, T. Suzuki, T. Otsuka, F. Xu, and N. Tsunoda, Phys. Rev. C **85**, 064324 (2012).
 [24] Y. Utsuno, T. Otsuka, B. A. Brown, M. Honma, T. Mizusaki, and N. Shimizu, Phys. Rev. C **86**, 051301 (2012).
 [25] T. Mizusaki, N. Shimizu, Y. Utsuno, and M. Honma, code MSHELL64 (unpublished).
 [26] K. Langanke, D. J. Dean, P. B. Radha, Y. Alhassid, and S. E. Koonin, Phys. Rev. C **52**, 718 (1995).
 [27] G. Audi and A. H. Wapstra, Nucl. Phys. A **595**, 409 (1995).
 [28] D. R. Bes and R. A. Sorensen, 'Advances in Nuclear Physics' (Plenum Press) vol. 2, 129 (1969).
 [29] Data extracted using the NNDC World Wide Web site from the ENSDF data base.
 [30] G. Kraus, *et al.*, Phys. Rev. Lett. **73**, 1773 (1994).
 [31] B. J. Cole, Phys. Rev. C **59**, 726 (1999).
 [32] R. Lüttke, *et al.*, Phys. Rev. C **85**, 017301 (2012).